

Early Miocene volcanic activity and paleoenvironment conditions recorded in tephra layers of the AND-2A core (southern McMurdo Sound, Antarctica)

A. Di Roberto¹, P. Del Carlo¹, S. Rocchi², and K.S. Panter³

¹*Istituto Nazionale di Geofisica e Vulcanologia, Sezione di Pisa, via della Faggiola 32, I 56126 Pisa, Italy*

²*Dipartimento di Scienze della Terra, Università di Pisa, Via S. Maria, 53, I-56126 Pisa, Italy*

³*Department of Geology, Bowling Green State University, Bowling Green, Ohio 43403, USA*

ABSTRACT

The ANtarctic geological DRILLing Program (ANDRILL) successfully recovered 1138.54 m of core from drill hole AND-2A in the Ross Sea sediments (Antarctica). The core is composed of terrigenous claystones, siltstones, sandstones, conglomerates, breccias, and diamictites with abundant volcanic material. We present sedimentological, morphoscopic, petrographic, and geochemical data on pyroclasts recovered from core AND-2A that provide insights on eruption styles, volcanic sources, and environments of deposition. One pyroclastic fall deposit, 12 resedimented volcanoclastic deposits and 14 volcanogenic sedimentary deposits record a history of intense explosive volcanic activity in southern Victoria Land during the Early Miocene. Tephra were ejected during Subplinian and Plinian eruptions fed by trachytic to rhyolitic magmas and during Strombolian to Hawaiian eruptions fed by basaltic to mugearitic magmas in submarine and/or subglacial to subaerial environments. The long-lived Mount Morning eruptive center, located ~80 km south of the drill site, was recognized as the probable volcanic source for these products on the basis of volcanological, geochemical, and age constraints. The study of tephra in the AND-2A core provides important paleoenvironment information by revealing that the deposition of primary and moderately reworked tephra occurred in a proglacial setting under generally open-water marine conditions.

INTRODUCTION

Over the past few decades significant insights on paleoenvironmental conditions in southern

Victoria Land have come from archives of sediments recovered in cores drilled both onshore and offshore (Barrett et al., 1998, 2000; Hambrey and Barrett, 1993; Fielding and Thomson, 1999; Naish et al., 2007; Harwood et al., 2008). The ANtarctic geological DRILLing Program (ANDRILL) successfully recovered sediments and geophysical data from 1138.54 m of drill core in the second AND-2A drill hole (southern McMurdo Sound; Florindo et al., 2008). The coring site is located in the Ross Sea, ~50 km northwest of Hut Point Peninsula on Ross Island (77°45.488'S; 165°16.613'E; Fig. 1).

The AND-2A core sampled an almost continuous (98% recovery) sequence of sediments composed of lithologies including terrigenous claystones, siltstones, sandstones, conglomerates, breccias, and diamictites (Florindo et al., 2008; Panter et al., 2008); 14 lithostratigraphic units were identified on the basis of major changes in lithology recognized during core description (Fielding et al., 2011). Sediments were interpreted to represent a wide and complex spectrum of depositional environments and dynamic fluctuations in the Antarctic ice sheet recorded in numerous cycles of glacial advance and retreat during the Early to Middle Miocene (Fielding et al., 2011; Passchier et al., 2011).

Results from ⁴⁰Ar/³⁹Ar radiometric dating of primary to moderately reworked tephra layers (Di Vincenzo et al., 2010) range in age from Early Miocene to Pleistocene (ca. 20 to ca. 0.08 Ma) and compose an expanded and almost continuous section of Early to Middle Miocene sediments (ca. 20–11.5 Ma) that has not been previously recorded by drilling in this region (Harwood et al., 2009).

We present sedimentological, morphoscopic, petrographic, and geochemical data from tephra recovered in the AND-2A core.

We also focus on some of the sedimentological aspects of the tephra in order to infer their depositional history. The results provide constraints on volcanic sources, eruptions styles, and depositional paleoenvironments.

EREBUS VOLCANIC PROVINCE

The Erebus volcanic province in southern Victoria Land represents the largest area of exposed late Cenozoic volcanic rocks and the most complete record of alkaline volcanism in Antarctica (Kyle and Cole, 1974; Kyle et al., 1990; Di Vincenzo et al., 2010). The Erebus volcanic province comprises several large volcanic centers built on the western flank of the intracontinental West Antarctic rift system in the McMurdo Sound region (Kyle et al., 1990) that range in age from the Early Miocene (ca. 19 Ma) to the present day (Fig. 1). Ross Island is the largest volcanic complex in the area and is formed by the active Mount Erebus volcano, which is surrounded radially by the Mount Terror, Mount Bird, and Hut Point Peninsula eruptive centers. Mount Erebus is composed mostly of basanite and phonolite deposits (Kyle, 1977, 1981; Kyle et al., 1992) that date to 1.3 Ma (basanite dike from Cape Barne; Esser et al., 2004). Mounts Bird and Terror are basanitic shield volcanoes that were active from 4.6 to 3.8 Ma and 1.7–1.3 Ma, respectively (Kyle et al., 1990; Kyle and Muncy, 1989). Hut Point Peninsula is Pleistocene in age (ca. 1.3 Ma), formed by alkaline volcanism, and is dominated by basanitic-hawaiitic cinder cones and a phonolite dome (Observation Hill) (Kyle, 1981).

To the south of Ross Island, the Erebus volcanic province is represented by White Island, a basanite to tephriphonolite shield volcano

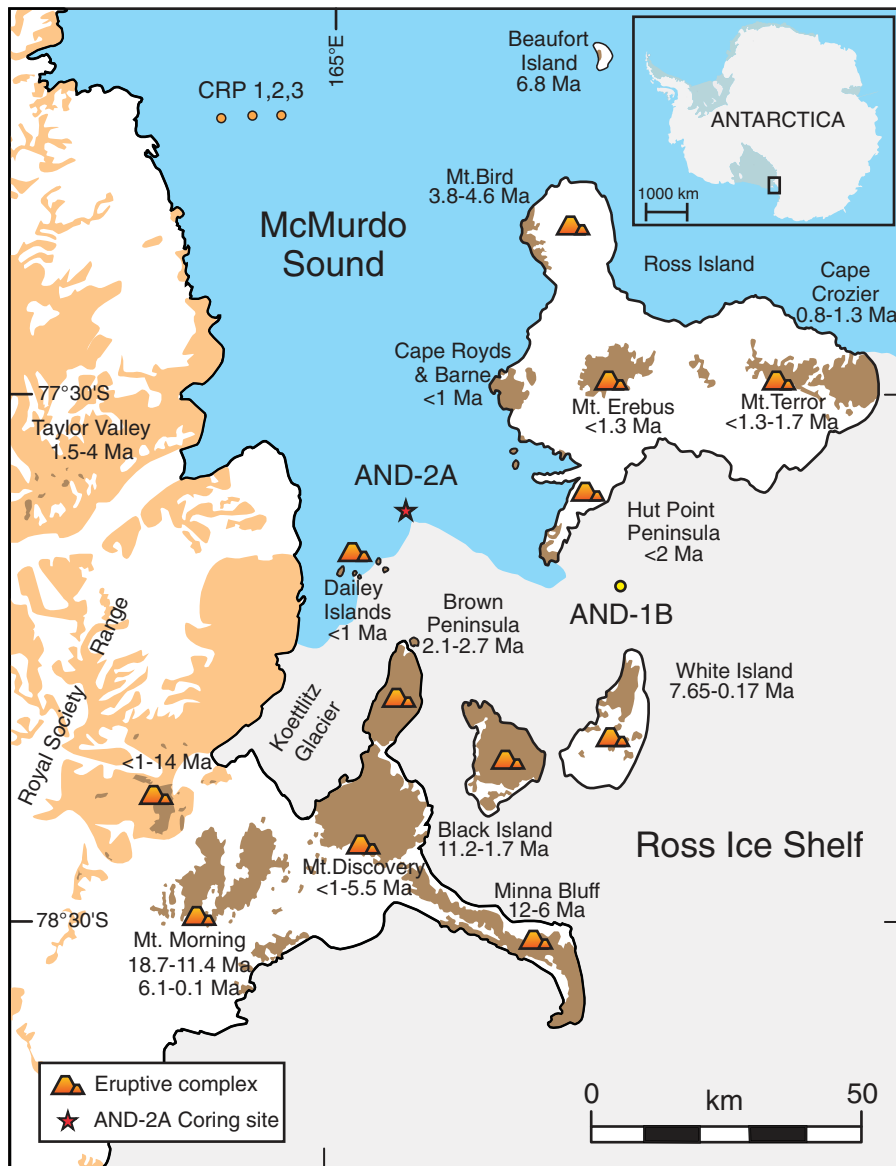


Figure 1. Map of southern Victoria Land, Antarctica, showing the location of AND-2A Southern McMuro Sound core site and relevant geological features of Erebus volcanic province. Map also shows outcrops of volcanic rocks (in dark brown) belonging to the McMuro Volcanic Group with relative time span of activity according to K-Ar and ^{40}Ar - ^{39}Ar ages (Mercer, 1968; Kyle and Cole, 1974; Mayewski, 1975; Armstrong, 1978; Kyle, 1981, 1982; Kyle et al., 1990; Kyle and Muncy, 1989; Wilch et al., 1993, 2008; Marchant et al., 1996; Esser et al., 2004; Tauxe et al., 2004; Timms, 2006; Cooper et al., 2007; Lewis et al., 2007; Paulsen and Wilson, 2009; Martin et al., 2010). CRP—Cape Roberts Project sites.

Erebus volcanic province and has been divided into two phases of activity. Phase I (18.7–11.4 Ma) is dominated by mildly alkaline, mostly trachytic rocks, and phase II (6.13–0.02 Ma) is composed of strongly alkaline rocks belonging to the basanite-phonolite lineage (Kyle and Muncy 1989; Wright-Grassham 1987; Kyle et al., 1990; Paulsen and Wilson, 2009; Martin, 2009; Martin et al., 2010).

North of Ross Island, Franklin and Beaufort Islands represent remnants of alkaline volcanic edifices, with ages that range from Quaternary (90 ± 66 ka; date from a seamount 10 km north of Franklin Island) to Late Miocene (6.80 ± 0.05 Ma) (Rilling et al., 2009). In addition to the large volcanic edifices, the Erebus volcanic province includes several small volcanic centers and fields (Kyle and Cole, 1974; Kyle et al., 1990). Numerous volcanic ash deposits are found within the hyperarid Dry Valleys region of the Transantarctic Mountains, chiefly in the Royal Society Range and the Wright and Taylor Valleys. Most of these volcanoclastic deposits were reported to be Miocene to Pliocene in age with $^{40}\text{Ar}/^{39}\text{Ar}$ ages ranging from ca. 15.15 to ca. 4.33 Ma (Kyle and Cole, 1974; Kyle et al., 1990; Marchant et al., 1996; Lewis et al., 2007). The Dailey Islands are ~10 km south of the Southern McMuro Sound drill site and consist of heavily eroded remnants of basaltic cinder cones and lava deposits. Studies of volcanic rocks from 2 of the 5 islands reveal paleomagnetic normal polarities and radiometric ages of 0.78 ± 0.04 Ma (Mankinen and Cox, 1988; Tauxe et al., 2004; Del Carlo et al., 2009). Traces of the earliest activity within the Erebus volcanic province come from volcanoclastic detritus and tephra recovered in the CIROS-1 (Cenozoic Investigations in the Western Ross Sea), MSSTS-1 (McMuro Sound Sediment and Tectonic Study), Cape Roberts Project, and AND-2A drill cores, which extend the volcanic history of the province back to ca. 26 Ma (Gamble et al., 1986; Barrett, 1987; McIntosh, 1998, 2000; Acton et al., 2008; Di Vincenzo et al., 2010).

VOLCANIC ROCKS IN AND-2A CORE AND ANALYTICAL METHODS

Preliminary stratigraphic and petrologic data on volcanic products in the AND-2A core were reported in Fielding et al. (2008) and Panter et al. (2008), and provide the foundation for this study. The volcanic material in the AND-2A core includes dispersed clasts of lava, scoria fragments, and pumices, variably reworked tephra layers, and one primary tephra. Of the total clasts identified in 9 of the 14 lithostratigraphic units (LSU), >50% are volcanic in

that was active as early as 7.65 Ma (Cooper et al., 2007). Evidence for Late Miocene (ca. 6.5 Ma) submarine to emergent volcanism was found in close proximity to White Island (Di Roberto et al., 2010). Farther south, Black Island, Minna Bluff, Mount Morning, and Mount Discovery are all major eruptive centers belonging to the Erebus volcanic prov-

ince. The Minna Bluff peninsula and Black Island volcanic complexes are both composed of alkaline volcanic products belonging to the basanite-phonolite lineage and were active between ca. 12 and 4 Ma (Fargo et al., 2008; Wilch et al., 2011) and between 11.2 and 1.7 Ma (Timms, 2006), respectively. Mount Morning is the oldest volcanic complex in the

origin and LSU 1 (0–37 m below seafloor, mbsf) represents the most volcanic-rich unit within the core. The weakly reworked tephra beds, lava breccias, and ripple cross-laminated vitroclastic sands in LSU 1 are interpreted to have been deposited in a shallow-marine environment by Strombolian- and Hawaiian-type volcanism from proximal volcanic sources (Del Carlo et al., 2009).

For this study, 27 volcanoclastic beds were identified and sampled from LSU 2 to LSU 14 (i.e., between 37.07 and 1138.54 mbsf; Fig. 2; Table 1) and their sedimentological and volcanological characteristics are the basis for the interpretations presented herein. Because most of these samples are poorly lithified, they were impregnated with epoxy resin and prepared as standard polished thin sections for petrography and electron microprobe analysis. Observations of the sediments and sedimentary rocks were made using a stereomicroscope in order to detail sedimentologic structures and qualitatively identify sediment components and their relative abundance. This work led to the selection of samples for scanning electron microscopy and analysis by electron microprobe. Morphological and textural observations of components were performed by means of scanning electron microscopy (SEM) at Istituto Nazionale di Geofisica e Vulcanologia (Sezione di Pisa) using a Zeiss EVO MA 10 equipped with an Oxford ISIS microanalysis system. Major element glass composition and mineral analyses of glass-bearing volcanic fragments and alteration phases were performed at the HPHT Laboratory of Istituto Nazionale di Geofisica e Vulcanologia (Sezione di Roma) using a JEOL JXA 8200 microprobe equipped with 5 wavelength-dispersive spectrometers and an energy-dispersive analyzer system. Instrumental conditions were accelerating voltage 15 kV, beam current 5 nA, probe diameter 5 μ m, and acquisition time 10 s and 5 s for peak and background, respectively. Whenever possible, at least 25 particles were analyzed in each sample. Relative standard errors for each element are reported in Supplemental Table 1¹.

RESULTS

The sampled deposits have been grouped into three types based on sedimentary features, the nature and abundance of components (Figs. 3 and 4), and on the major element compositions

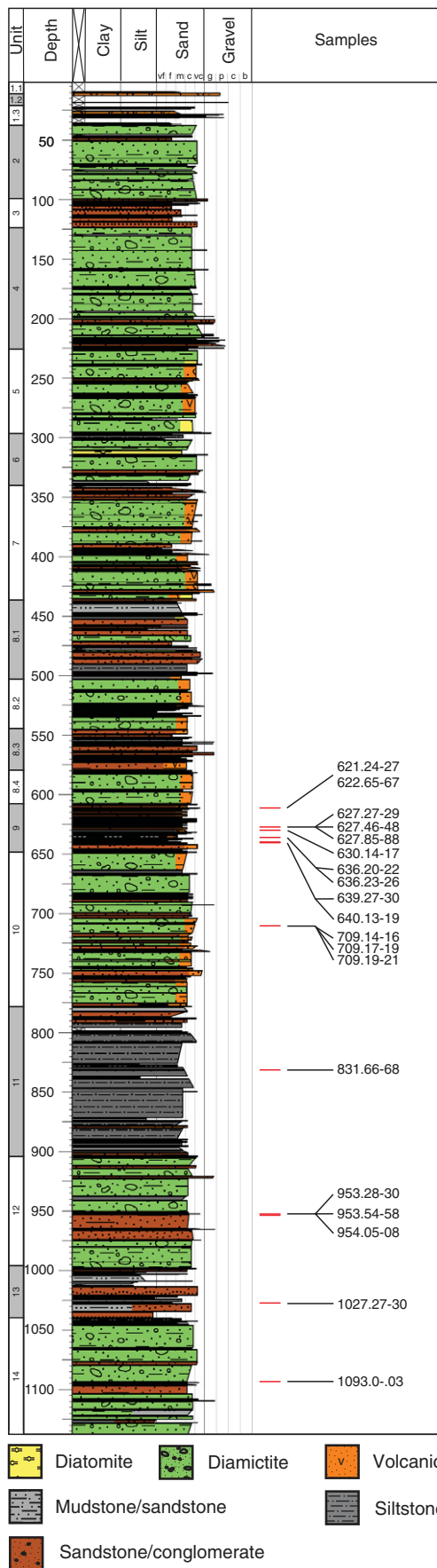
TABLE 1. DESCRIPTIONS OF ANALYZED SAMPLES

| Sample (AND 2A: depth mbsf) | LSU | Sediment type | Lithology | Glass composition (unaltered) |
|-----------------------------|-------|-----------------------------|--|---------------------------------|
| 621.24-27 | LSU 9 | Resedimented volcanoclastic | Resedimented pumice- and scoria-rich sandstone to lapillistone | Basanite to mugearite |
| 622.65-67 | LSU 9 | Volcanogenic | Shards-rich siltstone to sandstone | Basanite to mugearite |
| 627.27-29 | LSU 9 | Volcanogenic | Shards-rich siltstone to sandstone | Basalt to basanite to mugearite |
| 627.46-48 | LSU 9 | Volcanogenic | Shards-rich siltstone to sandstone | N/A |
| 627.85-88 | LSU 9 | Volcanogenic | Shards-rich siltstone to sandstone | Basanite to basalt |
| 630.14-17 | LSU 9 | Volcanogenic | Shards-rich siltstone to sandstone | Basanite to mugearite |
| 636.20-22 | LSU 9 | Resedimented volcanoclastic | Resedimented, laminated, ash-rich mudstone to sandstone | Basanite to basalt |
| 636.23-26 | LSU 9 | Resedimented volcanoclastic | Resedimented, laminated, ash-rich mudstone to sandstone | Basanite to mugearite |
| 639.27-30 | LSU 9 | Volcanogenic | Shards-rich siltstone to sandstone | Basanite to mugearite |
| 640.13-19 | LSU 9 | Pyroclastic deposit | Lapilli tuff | Basanite |
| 709.14-16 | LSU10 | Resedimented volcanoclastic | Resedimented pumice- and scoria-rich sandstone to lapillistone | Basanite to basalt |
| 709.17-19 | LSU10 | Resedimented volcanoclastic | Resedimented pumice- and scoria-rich sandstone to lapillistone | Basanite to basalt |
| 709.19-21 | LSU10 | Resedimented volcanoclastic | Resedimented pumice- and scoria-rich sandstone to lapillistone | Basanite to basalt |
| 831.66-68 | LSU11 | Resedimented volcanoclastic | Resedimented pumice- and scoria-rich sandstone to lapillistone | Basanite to basalt |
| 953.28-30 | LSU12 | Resedimented volcanoclastic | Resedimented pumice- and scoria-rich sandstone to lapillistone | Trachyte |
| 953.54-58 | LSU12 | Resedimented volcanoclastic | Resedimented pumice- and scoria-rich sandstone to lapillistone | Basanite |
| 954.05-08 | LSU12 | Resedimented volcanoclastic | Resedimented pumice- and scoria-rich sandstone to lapillistone | N/A |
| 1027.27-30 | LSU13 | Resedimented volcanoclastic | Resedimented, laminated, ash-rich mudstone to sandstone | Trachyte |
| 1093-03 | LSU13 | Resedimented volcanoclastic | Resedimented pumice- and scoria-rich sandstone to lapillistone | Trachyte |

Note: Ages are from Di Vincenzo et al. (2010); mbsf—meters below seafloor; LSU—lithostratigraphic unit; N/A—not available.

¹Supplemental Table 1. Relative standard error. If you are viewing the PDF of this paper or reading it offline, please visit <http://dx.doi.org/10.1130/GES00754.S1> or the full-text article on www.gsapubs.org to view Supplemental Table 1.

Volcanic activity and paleoenvironment conditions in tephra layers of the AND-2A core



of glassy fragments (Fig. 5; Table 2). They are: (1) pyroclastic fall deposits (P), (2) reseedimented volcanoclastic deposits (RV), and (3) volcanogenic sedimentary deposits (V; terminology after McPhie et al., 1993).

Pyroclastic Fall Deposit

A 6-cm-thick (between 640.13 and 640.19 mbsf) pyroclastic fall deposit was identified within LSU 9 (Panter et al., 2008; Di Vincenzo et al., 2010). The lapilli tuff is massive to faintly normally graded and contains a homogeneous distribution of pale green pumice fragments (<3 mm in diameter) set in matrix formed by angular glass shards that range in size from coarse to very fine ash. The lapilli tuff is underlain and overlain by volcanic-rich sandstones composed of light brown fresh volcanic glass shards, pale green to white altered glass shards, abundant lithic fragments (commonly of metasandstones and schists and less commonly of granite, dolerite, and marble) and loose crystals (mainly quartz and alkali and plagioclase feldspars).

The contact with the underlying sediment is sharp, whereas the upper contact is gradational (Fig. 3A). Pale green pumices are moderately to highly vesicular (Houghton and Wilson, 1989) with a frothy morphology. Vesicles range in shape from spherical to elongated and are sometimes deformed (collapsed) or highly coalesced. Pumices are mostly aphyric with rare K-feldspar phenocrysts (<2 mm) occasionally occurring with strongly colored green clinopyroxene (<1 mm; optically determined aegirine or aegirine-augite). Angular glass shards are usually blocky, vesicle free to poorly vesicular with vesicles ranging in shape from spherical to oblate (collapsed). A continuous spectrum of vesicularity exists between vesicle-free glass shards and highly vesicular pumice. Glass fragments forming the fine-grained part of the deposit (very fine ash) are variably vesicular (analogous to those described above) and range in shape from y-shaped to cusped and blocky (Fig. 4A).

Most of the analyzed glass shards and pumice fragments are subtly to weakly altered with thin (<3 μm) transparent rims of leached glass at the surface of the grains and along fractures and vesicles (Fig. 4E). Well-developed pervasive perlitic fractures occur chiefly in dense,

Figure 2. Stratigraphic summary of the AND-2A core with lithologies plotted against depth. Studied samples are also reported. Abbreviations: vf—very fine; f—fine; m—medium; c—coarse; vc—very coarse; g—granule; p—pebble; c—cobble; b—boulder.

angular glass fragments (Fig. 4F). The deposit is cemented by calcite and clay minerals.

Resedimented Volcaniclastic Deposits

We identified 12 resedimented volcaniclastic deposits (defined in accordance with McPhie et al., 1993) between 621.24 and 1093 mbsf (LSU 9–13; Table 1). Two groups were distinguished within these deposits: (1) resedimented pumice- and scoria-rich sandstone to lapillistone (9 layers; Fig. 3B), and (2) resedimented, strongly laminated, ash-rich mudstone to sandstone (3 layers; Fig. 3C). Resedimented pumice- and scoria-rich sandstone to lapillistone compose grain-supported, <2 cm beds and lenses of pale green and clear, highly vesicular pumice mixed with scoria clasts made up of variably vesicular (from dense to pumiceous), light to dark yellow sideromelane and tachy-

lite fragments (Fig. 4B). Clasts occur in a fine sand matrix, which is cross-laminated to parallel-laminated at scales of millimeters to centimeters. The matrix is composed of glass fragments with the same range of composition as the clasts, with crystals of K-feldspar, plagioclase, quartz, and lithic fragments (metasandstones and schists, and less commonly granite, dolerite, and marble; Fig. 4B). Pumice and scoria fragments are in some cases abraded and subrounded. Deposits have sharp and planar contacts with the underlying sediments, whereas upper contacts are gradational to diffuse; fragments with elongated shapes are commonly imbricated parallel to sand laminae or oriented along the lee side of ripple cross-laminations. Pumice are similar in vesicularity, alteration degree (subtle to weak), and texture to those observed in the pyroclastic fallout deposit at 640.13–640.19 mbsf (Fig. 4A); they

are mostly aphyric with minor K-feldspar phenocrysts (<2 mm), and rarely accompanied by (<1 mm) strongly colored green clinopyroxene (optically determined aegirine or aegirine-augite). A second population of pumice and glass shards, with textures similar to those previously described but made of clear glass, was identified in 5 samples at 831.68, 953.28, 954.05, 1027.27, and 1093 mbsf, and rarely within sediments at shallower depths. Scoria clasts and light to dark yellow sideromelane and tachylite fragments are pumiceous to blocky to y-shaped (Figs. 3B and 4B). The scoria is weakly porphyritic with microphenocrysts of plagioclase, rare strongly colored green clinopyroxene, and minor olivine, apatite, and magnetite set in a hypocrySTALLINE groundmass. Glass is pristine to subtly altered with rims of palagonite to smectite a few micrometers thick that line clasts or vesicles walls.

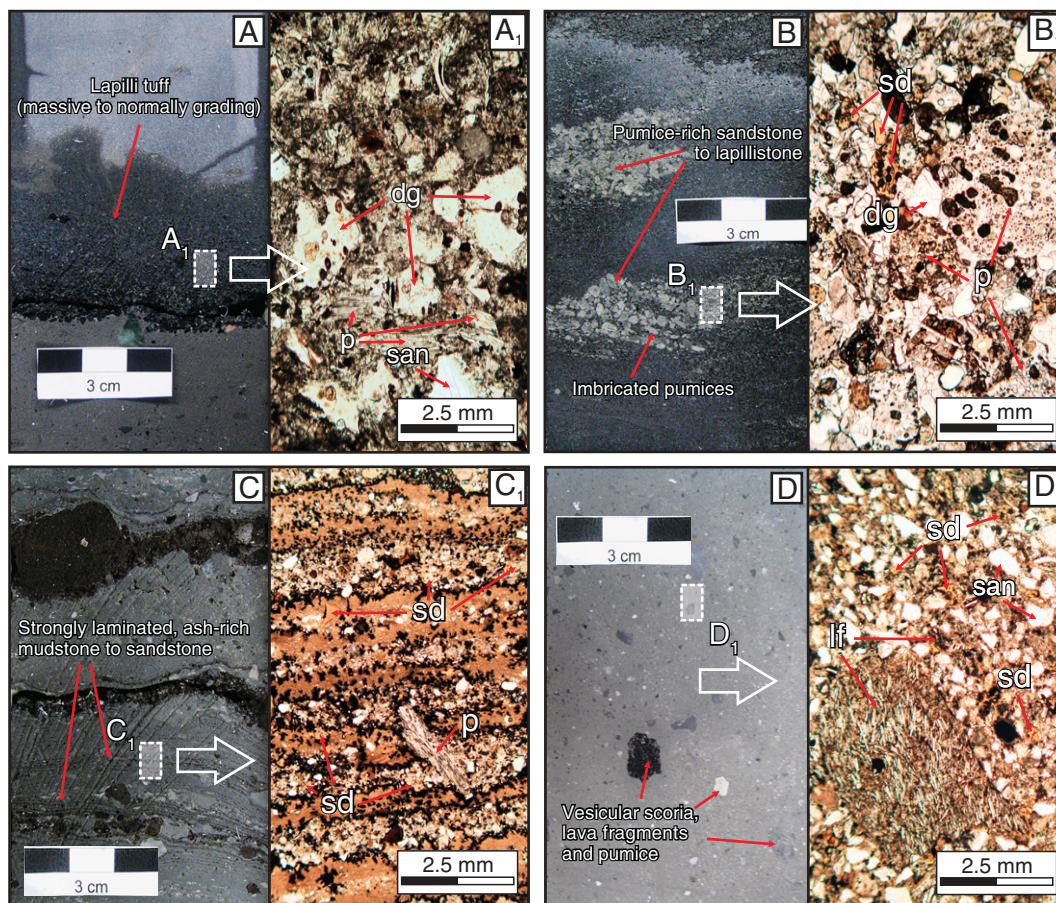


Figure 3. Core (left columns) and thin section optical microscope images (right columns) representative of the four main volcaniclastic sediment types identified in the AND-2A core. Abbreviations: dg—dense glass; lf—lava fragment; p—pumice; san—sanidine; sd—sideromelane. (A) Pyroclastic fall deposit (640.13 m below seafloor, mbsf). (B) Resedimented pumice- and scoria-rich sandstone to lapillistone (709.13 mbsf). (C) Resedimented, strongly laminated, ash-rich mudstone to sandstone (636.23 mbsf). (D) Shard-rich mudstones and sandstones (712.04 mbsf).

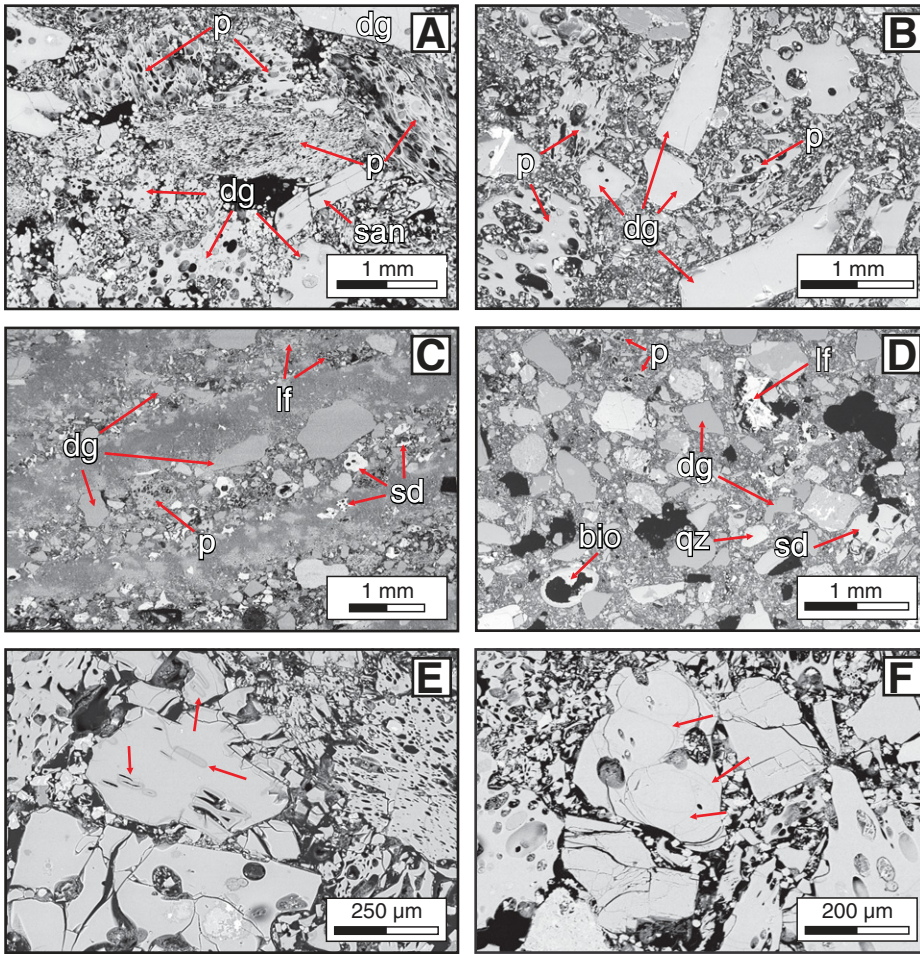


Figure 4. Scanning electron microscope back-scattered images representative of the four main volcaniclastic sediment types identified in AND-2A core. Abbreviations: dg—dense glass, p—pumice, bio—bioclast, lf—lava fragment, qz—quartz, san—sanidine, sd—sideromelane. (A) Pyroclastic fall deposit. (B) Resedimented pumice- and scoria-rich sandstone to lapillistone. (C) Resedimented, strongly laminated, ash-rich mudstone to sandstone. (D) Shard-rich mudstones and sandstones. (E) Rims of leached glass occurring at the surface of the grains along fractures and vesicles (red arrows). (F) Pervasive perlitic fractures occurring chiefly in glass shards and in the least vesicular fragments (red arrows).

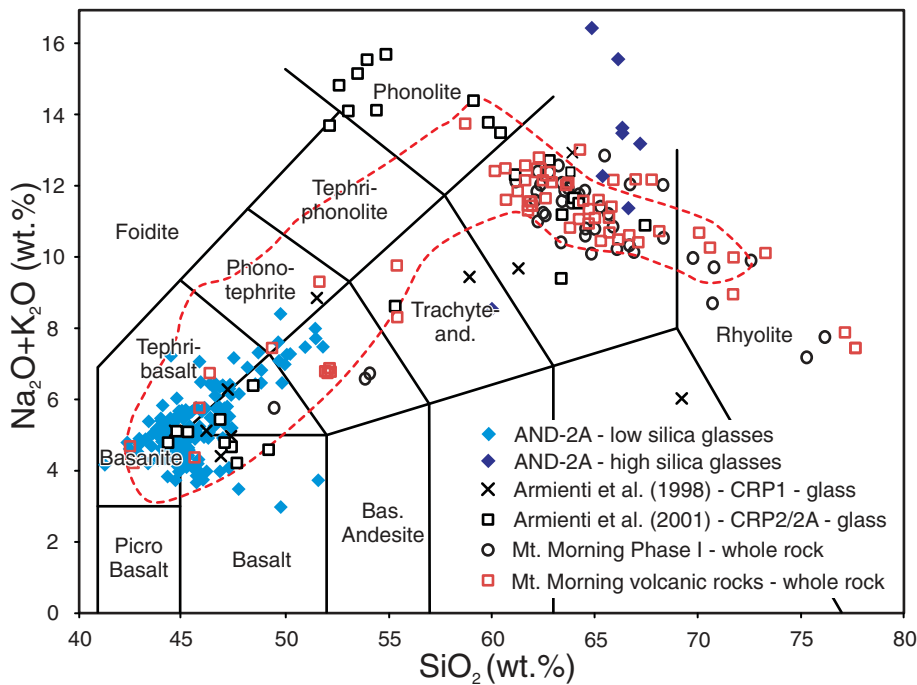


Figure 5. Total alkali versus silica diagrams from LeMaitre (1989) for unaltered AND-2A glass compositions (blue diamonds). For comparison between composition of glasses in AND-2A and Erebus volcanic province products (red dashed curve; Armienti et al., 1998, 2001), glass composition of fragment recovered in CRP1 (Cape Roberts Project), CRP2/2A (Armienti et al., 1998, 2001), volcanic products of the phase I activity of Mount Morning (Martin et al., 2010), and Mount Morning volcanic rocks (Muncy, 1979; Wright-Grassham, 1987; Martin et al., 2010) are also reported.

TABLE 2. CHEMICAL COMPOSITIONS OF ANALYZED VOLCANIC GLASS

| Sample | 621.24-22 | 636.20-22 | 636.23-26 | 640.13-19 | 709.14-16 | 709.17-19 | 709.19-21 | 831.66-68 | 953.56-58 | 1027.27-30 | 1093-03 |
|--------------------------------|-----------|-----------|-----------|-----------|-----------|-----------|-----------|-----------|-----------|------------|---------|
| SiO ₂ | 43.80 | 51.50 | 42.96 | 46.11 | 42.86 | 48.19 | 42.63 | 48.58 | 44.90 | 59.42 | 66.56 |
| TiO ₂ | 4.16 | 3.01 | 3.80 | 3.24 | 4.27 | 3.27 | 5.52 | 3.68 | 4.00 | 0.05 | 0.19 |
| Al ₂ O ₃ | 15.25 | 15.35 | 14.86 | 16.24 | 14.83 | 15.78 | 13.19 | 13.73 | 15.93 | 24.24 | 30.84 |
| FeO ^{tot} | 12.49 | 10.34 | 11.92 | 10.15 | 12.85 | 10.09 | 12.33 | 12.91 | 10.82 | 11.45 | 15.90 |
| MnO | 0.14 | 0.27 | 0.19 | 0.21 | 0.18 | 0.15 | 0.24 | 0.23 | 0.25 | 0.28 | bdl |
| MgO | 5.61 | 3.36 | 5.38 | 4.81 | 5.54 | 3.31 | 5.13 | 5.62 | 3.84 | 3.11 | bdl |
| CaO | 10.87 | 7.04 | 10.93 | 10.23 | 10.89 | 6.81 | 9.87 | 11.26 | 7.62 | 11.15 | 9.87 |
| Na ₂ O | 3.82 | 5.04 | 3.49 | 4.36 | 3.83 | 4.86 | 4.07 | 3.43 | 4.53 | 3.47 | 11.51 |
| K ₂ O | 1.35 | 2.67 | 1.25 | 2.08 | 1.35 | 2.61 | 1.70 | 1.10 | 2.36 | 1.14 | 14.91 |
| P ₂ O ₅ | 1.50 | 1.09 | 1.56 | 1.19 | 1.38 | 1.18 | 0.99 | 1.61 | 1.42 | 1.63 | 0.33 |
| Total | 98.99 | 99.66 | 96.32 | 98.87 | 99.00 | 98.45 | 99.79 | 98.65 | 97.95 | 98.12 | 99.38 |
| Alkali | 5.17 | 7.71 | 4.74 | 6.44 | 5.18 | 7.47 | 5.77 | 4.53 | 6.90 | 4.61 | 13.05 |

Note: Values shown are the highest and lowest SiO₂ contents with a given sample. Chemical compositions of samples at 627.46-48 and 954.05-08 (m below seafloor) were not reported because they are entirely formed by altered glass shards. bdl—below detection limit.

Resedimented, strongly laminated, ash-rich mudstone to sandstone consist of parallel laminated, rhythmic couplets of grain-supported fine sandstone to siltstone grading upward to mudstone. Couplets range in thickness from <1 mm to a few millimeters. Individual couplets have sharp lower and upper contacts whereas internal contacts between the volcanoclastic silt, sand, and clay facies range from gradational to sharp (Figs. 3C and 4C). Volcanoclastic silt and fine sand laminae are composed of pale green, highly vesicular pumice fragments mixed with dense to pumiceous, light brown sideromelane and tachylite fragments. Fragments are pristine and preserve thin vesicle glass walls and fragile structures. Minor amounts of loose crystals (<1 mm) of K-feldspar, plagioclase, quartz, and lithics (commonly mafic lava fragments, granite dolerite, and rarely schists) are present. Lapilli-sized pumice fragments and sedimentary intraclasts (siltstone) are observed to load underlying clay laminae and to be draped by laminae at the top.

Volcanogenic Sedimentary Deposits

Volcanogenic sedimentary deposits, i.e., shard-rich mudstones and sandstones (McPhie et al., 1993), were identified at several depths (LSU 2-13; Table 1). This type of deposit includes intervals of <2 mm, variably vesicular scoria and pale green and clear pumice set in sand- to silt-sized volcanic-rich matrix. Abundant lithic fragments (Figs. 3D and 4D) of most commonly volcanic rocks are recorded; they are mainly represented by variably vesicular lava with feldspar and <2 mm, strongly colored green clinopyroxene (optically determined aegirine or aegirine-augite) set in an intergranular to felted groundmass. Crystals of quartz, K-feldspar, and biotite are present. Palagonitized glass shards and vesicular fragments were found in some samples. Rare, holocrystalline intrusive rocks are found that consist mainly of granitoids (quartz ± feldspar ± biotite ± hornblende) with hypidiomorphic to allotriomorphic and moderately deformed textures. Rare metamorphic lithic fragments consisted of schist, gneiss, quartzite, and low-grade metasediments. Bioclasts are common and include foraminifera, shell fragments, spicules, diatoms, and bryozoans (Fig. 4D). Regardless of their origin (volcanic, metamorphic, or biologic), fragments within vitric siltstone and sandstone are usually subrounded to well rounded. Lithologies of lithic fragments are similar to those of clasts described for the same interval (for more detail descriptions of their characteristics and inferences on their provenance, see Panter et al., 2008; Talarico et al., 2011).

Below 953.28 mbsf, the majority of glass fragments forming the volcanogenic sedimentary deposits are moderately to strongly altered. Most of the original textures have been modified or destroyed and volcanic glass is usually dissolved and replaced clay minerals, zeolites, and carbonates. In some samples pseudo-fiamme clasts are common and are interpreted to have formed from burial compaction of lapilli-sized pumice clasts. Diffuse authigenic pyrite is found together with frambooidal agglomerates of microscopic (<1 μm) isometric crystals of greigite (Fe₃S₄).

Chemistry of Volcanic Glass

We analyzed 600 glass fragments collected from throughout the length of the core (Table 2; Supplemental Fig. 1²). The SiO₂ contents of glass range from ~40 to ~73 wt% and have been divided into two main compositional groups: (1) light brown sideromelane and tachylite fragments with SiO₂ concentrations <52 wt% and (2) pale green to colorless glass fragments with SiO₂ >63 wt%. The majority of glass fragments within the second group are subtly to weakly altered and have low total oxides (<97 wt%).

The effects of alteration on the chemistry of volcanic glass is examined semiquantitatively by plotting their compositions in the alteration box plot (Large et al., 2001) shown in Figure 6. The diagram combines the alteration index (AI) of Ishikawa et al. (1976) and the chlorite-carbonate-pyrite index (CCPI) of Large et al. (2001), and was originally used with whole-rock compositional data in volcanic-hosted massive sulfide deposits to discriminate hydrothermal alteration mineral assemblages from diagenetic assemblages. When used in combination with other compositional data and detailed petrographic and textural observations, the alteration box plot gives an indication of alteration trends and processes.

Most of the low silica (52-63 wt% SiO₂), light brown sideromelane and tachylite fragments found within all sediment types within the depth interval between 621.24 and 831.68 mbsf are pristine and plot within the

²Supplemental Figure 1. Total alkali versus silica diagram (TAS; after LeMaitre, 1989) for analyzed AND-2A glass fragments. In the diagram, all glass compositions are plotted without any filtering for compositions of altered fragments. Filled symbols: fresh glass compositions; open symbols: altered glass compositions. If you are viewing the PDF of this paper or reading it offline, please visit <http://dx.doi.org/10.1130/GES00754.S2> or the full-text article on www.gsapubs.org to view Supplemental Figure 1.

least-altered rocks fields of the alteration box plot (light blue diamonds in Fig. 6). A few compositions are marked by a decrease of the CCPI values (depletion of FeO + MgO versus Na₂O + K₂O; pink diamonds in Fig. 6) and likely indicate incipient hydrothermal alteration. Below 831.68 mbsf, the alteration of light brown sideromelane and tachylite fragments increases further downcore, with glass being progressively replaced by zeolites and clay minerals and glass shards destroyed by compaction and diagenetic processes.

Throughout the core, the majority of the high silica (>63 wt% SiO₂), pale green to colorless glass fragments is subtly to weakly altered. Above ~953 mbsf, the glasses show homogeneous AI values ranging between ~40 and ~55, whereas values of CCPI vary more

broadly between ~35 and ~70 (red diamonds in Fig. 6). This indicates a rough increase of the CCPI values with respect to the relatively least altered rocks (depletion of Na₂O + K₂O versus FeO + MgO), which is typical of hydrothermal alteration in the chlorite-dominated zone (Large et al., 2001). Below ~953 mbsf to the bottom of the core, glass compositions spread along the lower margin of the diagram having low CCPI values (<20) and a wide range of AI values (~15–80; purple diamonds in Fig. 6).

Most of the pale green to colorless glass fragments that were initially considered unaltered (trachytic composition) plot across the lower margin of the alteration box plot. Despite their high total oxides (>97 wt%), they are interpreted to be subtly altered based on the slight depletion

in FeO + MgO and variable depletion in Na₂O + K₂O + CaO (blue diamonds in Fig. 6).

The unaltered light brown sideromelane and tachylite fragments range from basanite and basalt and/or tephrite to mugearite and overlap compositions of other basic volcanic rocks from the Erebus volcanic province (Fig. 5).

It is noteworthy that the pyroclastic fall deposit and resedimented volcanoclastic deposits have a narrow range of AI and CCPI values, whereas the volcanogenic sedimentary deposits show a broader range of values for these alteration indices. This could be attributed to the origin of each deposit type. For example, the pyroclastic fall deposit and resedimented volcanoclastic deposits are considered to be composed of fragments emitted from the same source, transported together and deposited contemporaneously. Alternatively, the volcanogenic sedimentary deposits may be a composite of products from multiple volcanic sources, with different transport and deposition dynamics, and thus should show greater variability in their degree of alteration.

Factors influencing the alteration of volcanic glass include the nature of the aluminosilicate source material (e.g., glass versus crystalline materials), the composition of original rock and pore fluids, the pH, the temperature, and porosity of sediments. None of these factors explains why felsic glass shards dispersed within sediments are more altered than the coexisting basaltic ones. Felsic glass is considered to alter at a slower rate relative to mafic glass. The alteration seems to be related to the glass viscosity, which in turn is a function of the composition and in particular H₂O and SiO₂ content (Gifkins et al., 2005, and reference therein). A possible explanation for why the basaltic glass is better preserved may be related to differences in the quenching (cooling) and hydration history of mafic versus felsic magmas (Marsaglia and Tazaki, 1992). Felsic magmas erupted in a water-rich environment (i.e., transitional or shallow water and subglacial) might have hydrated and altered more quickly than basaltic glass emitted in a water-free (subaerial) environment.

DISCUSSION

Eruptive Styles

The grain morphology, texture, and vesicularity of pyroclasts are indicative of eruptive style and the environment in which the eruption occurred. Magmatic eruptions typically produce variably vesicular particles with cusped to frothy morphologies, determined by viscosity, temperature, and volatile content (Cashman et al., 2000; Morrissey et al., 2000;

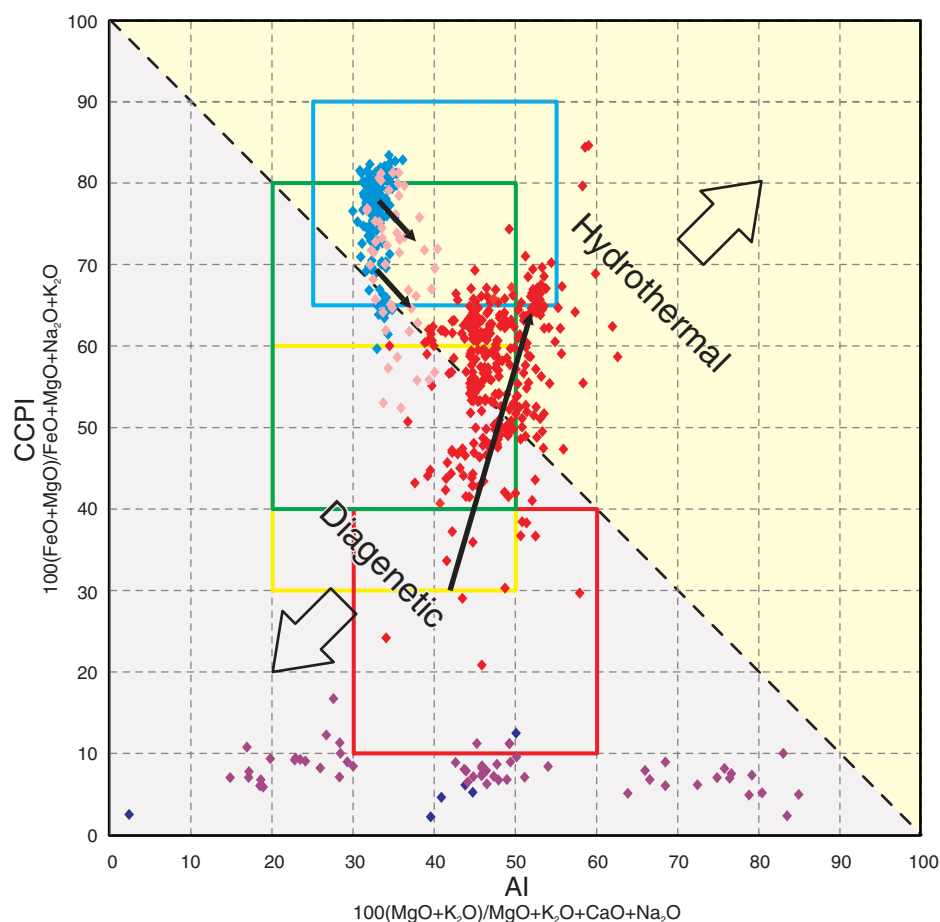


Figure 6. AI–CCPI (alteration index–chlorite-carbonate-pyrite index) alteration box plot diagram from Large et al. (2001) for analyzed AND-2A glass fragments. Data show different degrees and styles of alteration within studied samples. Colored rectangles identify least altered boxes for unaltered rocks with <52 wt% SiO₂ (blue rectangle), 52–63 wt% SiO₂ (green rectangle), 63–69 wt% SiO₂ (yellow rectangle), and >69 wt% SiO₂ (red rectangle). Solid symbols represent the compositions of unaltered glass (low silica in blue and high silica in navy blue) and altered glass (low silica in red and high silica in magenta), respectively, within the same sample.

Maria and Carey, 2002). Conversely, phreatomagmatic eruptions produce dense to poorly vesicular, often fine-grained (<100 μm) particles with a predominance of blocky morphologies (Cashman *et al.*, 2000; Morrissey *et al.*, 2000; Maria and Carey, 2002). Primary volcanic particle morphology can then be affected by post-eruptive reworking. Volcanic particles identified in the AND-2A core show a variety of morphologies and range from vesicle free to highly vesicular, suggesting that they were formed from both magmatic and phreatomagmatic eruptions under a range of conditions, detailed in the following.

High-Silica Glass

The morphology and texture of highly vesicular pumice within the pyroclastic fall deposit and resedimented volcanoclastic deposits in the AND-2A core are indicative of magmatic fragmentation processes. These products are emitted during energetic Subplinian and Plinian eruptions fed by silicic magmas. During these eruptions large amounts of highly vesicular pumice (60–93 vol%; Klug and Cashman, 1996; Cashman *et al.*, 2000) and fine ashes are produced and carried in eruptive columns as much as several tens of kilometers high and dispersed by winds distances to hundreds of kilometers from the source (Carey and Bursik, 2000).

In contrast, dense to poorly vesicular, fine-grained glass shards, with a predominance of blocky morphologies and hydration cracks and perlitic fracturing textures, suggest phreatomagmatic fragmentation processes (Heiken and Wohletz, 1985, 1991; Houghton and Wilson, 1989). Phreatomagmatic eruptions may occur in submarine and sublacustrine environments, or when magma comes into contact with groundwater or wet sediment (Heiken and Fisher, 2000). In glacial marine environments like McMurdo Sound, the most likely water sources for phreatomagmatic process are seawater and ice (Smellie, 2000).

Despite strong differences in morphology and vesicularity, the highly vesicular pumice and dense to poorly vesicular glass fragments have the same chemical composition (and degree of alteration) and coexist within the same layer, indicating that they may represent different fragmentation processes (magmatic versus phreatomagmatic) within a single eruption. In addition, as described herein, there is a continuum between end-member types covering the entire spectrum of vesicularity within these layers. This is consistent with a volcanic eruption occurring in a transitional environment, *i.e.*, evolving from shallow-water or subglacial conditions (strong magma-water interaction) to a subaerial environment (no magma-water inter-

action). Alternatively, multiple vents located in subaerial and shallow subaqueous environments or a single vent undergoing rapid cycling between dry Strombolian and wet phreatomagmatic explosions during a single eruptive phase (Panter and Winter, 2008) may be invoked.

Low-Silica Glass

Sideromelane and tachylite fragments are frothy, blocky, y-shaped, or cusped, and vary from vesicle free to highly vesicular. Most of the vesicular scorias observed are typical of weakly to mildly explosive Strombolian- or Hawaiian-style eruptions (Cashman *et al.*, 2000). Strombolian eruptions consist of rhythmic, usually short-lived, mildly energetic explosions during which magmatic volatiles are released and significant amounts of ash- to bomb-sized materials are ejected to heights of a few hundred meters above a crater. Hawaiian style eruptions involve lava flows together with lava fountains, typically tens to hundreds of meters in height. Typically lava fountains are fed by basaltic magmas characterized by low viscosity, low volcanic gas content, and high temperature. Lava fountains eject pyroclasts ranging in size from millimeters to ~1 m in diameter (Parfitt, 2004). Pyroclasts formed during Strombolian- and Hawaiian-style eruptions accumulate mainly as coarse, primary fallout deposits within a few kilometers of the vent. Only in the rare cases of strong magmatic fragmentation, for example during violent Strombolian or Plinian basaltic eruptions, can pyroclasts be dispersed hundreds of kilometers from the source.

As with high-silica glasses, the presence of basaltic particles that are dense to poorly vesicular and fine-grained with blocky morphologies in AND-2A pyroclastic fall and resedimented volcanoclastic deposits may indicate phreatomagmatic activity.

Volcanic Source

Major element compositions of glass fragments combined with $^{40}\text{Ar}/^{39}\text{Ar}$ age data from the pyroclastic fall deposit and resedimented volcanoclastic deposits (see Table 1; age data from Di Vincenzo *et al.* 2010) provide information on the provenance of volcanic materials. The ages of studied AND-2A samples vary from ca. 20–17.11 Ma (Early Miocene), according to $^{40}\text{Ar}/^{39}\text{Ar}$ age determinations of Di Vincenzo *et al.* (2010). Volcanic activity of comparable age occurred on the Malta Plateau in the Melbourne volcanic province (Armienti *et al.*, 1991; Müller *et al.*, 1991) and in the Erebus volcanic province at Mount Morning (Wright-Grassham, 1987; Kyle and Muncy, 1989; Kyle *et al.*, 1990; Martin *et al.*, 2010). In the Melbourne volcanic

province, Middle Eocene magmatic activity is preserved in the form of multiple intrusions dated as 47.5 and 38.6 Ma (Tonarini *et al.*, 1997; Rocchi *et al.*, 2002). The oldest subaerial volcanic rocks that crop out at Malta Plateau and Deception Plateau are dated as ca. 15 and 14 Ma (Armienti and Baroni, 1999). Dikes at Malta Plateau, possibly feeding lava flows, are dated as between ca. 18.2 and 14.1 Ma (Schmidt-Thomé *et al.*, 1990). Although similar in composition and age, it is highly unlikely that Early to Middle Miocene volcanism in northern Victoria Land (Malta Plateau) is the source for AND-2A deposits, simply because this activity occurred more than 500 km north of the drill site and the predominate wind and ice paleodirections are inferred to have been in a northward direction in McMurdo Sound area (Sandroni and Talarico, 2006; Talarico and Sandroni, 2011). It is more likely that the volcanic source was to the south of the drill site. The oldest Erebus volcanic province rocks crop out at Mount Morning, where $^{40}\text{Ar}/^{39}\text{Ar}$ and K-Ar ages indicate that activity occurred in two phases: the first one between at least 18.7 and 11.4 Ma and the second one between 6.13 and 0.02 Ma (Paulsen and Wilson, 2009; Martin, 2009; Martin *et al.*, 2010). Evidence of volcanic activity predating the onset of documented Mount Morning volcanism was found in volcanoclastic detritus and tephra beds recovered in CIROS-1, MSSTS-1, and Cape Roberts (CRP) drill cores. The dates on these materials extend activity within the Erebus volcanic province back to ca. 26 Ma (Gamble *et al.*, 1986; Barrett, 1987; McIntosh, 1998, 2000; Acton *et al.*, 2008; Di Vincenzo *et al.*, 2010). Volcanic activity older than ca. 19 Ma can be ascribed to either a proto-Mount Morning volcano buried under the present-day Mount Morning edifice, or to an unknown volcanic center, which has been eroded away or buried (Martin *et al.*, 2010).

In Figures 5 and 7, major element compositions of glass fragments from the AND-2A core are compared with those of Early to Middle Miocene products sampled on land or in drill cores and attributed to the Erebus volcanic province (Armienti *et al.*, 1998, 2001; Pompilio *et al.*, 2001; Kyle, 1981; Smellie, 1998). Only a limited number of glass compositions are available for McMurdo volcanics and the majority of data is from whole rocks. Nevertheless, the available data indicate that there is strong similarity between compositions of glass fragments in AND-2A core and some compositions of glass shards from volcanoclastic detritus and tephra beds recovered in CRP2/2A drill cores, which has already been attributed to the activity of the Erebus volcanic province (Armienti *et al.*, 1998 and 2001;

Smellie, 1998) and most likely sourced from Mount Morning. Discrepancies in the $\text{FeO}_{\text{total}}$ content between CRP2/2A drill core glasses and AND-2A core glass may be caused by minor alteration of the latter, as indicated by the alteration box plot (Figs. 4 and 7).

According to Martin (2009) and Martin et al. (2010), only 7% of Mount Morning phase I products sampled are mafic, whereas the remainder are felsic, specifically trachyte (79%) and rhyolite (14%) in composition. Our work and ongoing studies on sediments from different depth intervals (Nyland, 2011; Nyland et al., 2011) indicate that mafic glass is abundant throughout the AND-2A core. The fresh mafic glass have alkali basalt, basanite, tephrite, and (less commonly) mugearite compositions (Fig. 5), overlapping those of McMurdo Volcanic Group igneous products (Fig. 5; Kyle et al., 1990; Armienti et al., 1998; Rocchi et al., 2002; Nardini et al., 2009). At depths >600 mbsf the SiO_2 content of glass increases with increasing depth (Fig. 8). Unaltered basaltic compositions

occur prevalently above ~800 mbsf; below this depth they are altered and replaced by clay minerals and zeolites. Glass compositions below ~840 mbsf show a shift toward higher SiO_2 contents, the highest (~70 wt%) occurring near the bottom of the core (Fig. 8).

Our results complement the findings of Martin (2009) and Martin et al. (2010), confirming the bimodal compositions of Mount Morning products. However, we found that abundance of basaltic glass in the AND-2A core to be much higher than the 7% estimated for Mount Morning deposits. This suggests that during the period corresponding to phase I activity at Mount Morning, volcanism fed by mafic magmas was much more prevalent than previously documented in surface deposits. This discrepancy may be explained by the premise that present-day exposures on Mount Morning may not be representative of all of the material erupted. It could well be that Miocene trachyte and rhyolite deposits on Mount Morning, consisting

of remnants of domes and welded pyroclastic flows, were more resistant to weathering and erosion than basaltic scoria or even basaltic lava flows.

On the basis of textural and geochemical information we can infer eruption dynamics and sources. Given that almost all studied samples consist of particles produced by a combination of subaerial and submarine and/or subglacial magmatic and phreatomagmatic explosive activity (i.e., highly vesicular pumice, basaltic vesicular scoria, and vesicle-free blocky fragments), we suggest three possible scenarios: (1) a single volcanic complex, set in a transitional environment (submarine and/or subglacial to subaerial) erupting products with bimodal composition (basaltic and trachytic-rhyolitic); (2) two contemporaneously active volcanic complexes, both set in a transitional environment (submarine and/or subglacial to subaerial) and fed separately by basaltic and trachytic-rhyolitic magmas; (3) multiple contemporaneously active volcanic vents located

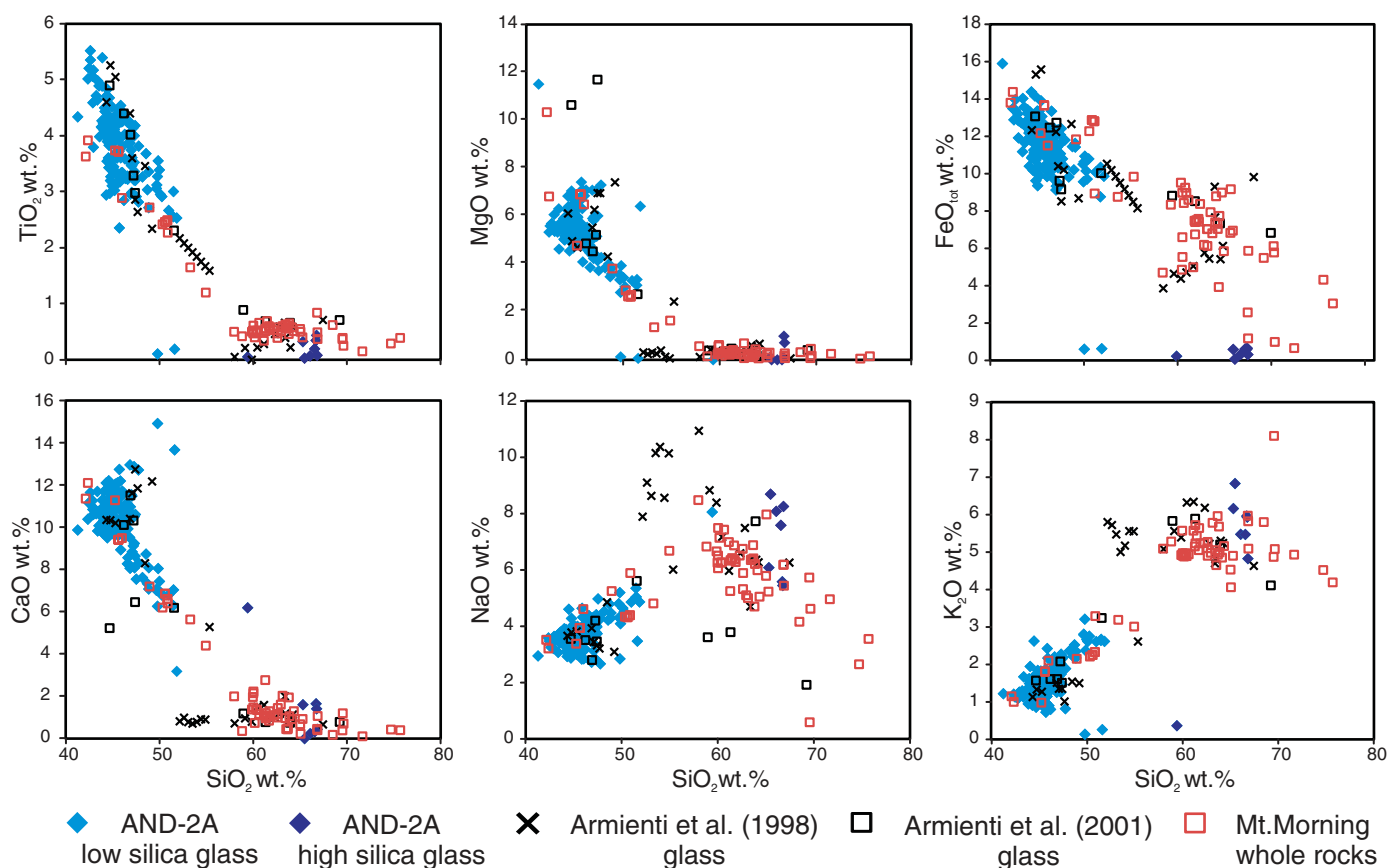


Figure 7. Harker diagrams for unaltered AND-2A glass shards (blue diamonds). Glass compositions are compared with the compositions of glass fragments recovered in CRP1 (Cape Roberts Project; black x symbols), CRP2/2a drill cores (black squares), and those attributed to proto-Mount Morning and Mount Morning activity (Armienti et al., 1998, 2001). Whole-rock compositions of Mount Morning volcanic rocks (Muncy, 1979; Wright-Grassham, 1987; Martin et al., 2010) are also reported (red squares).

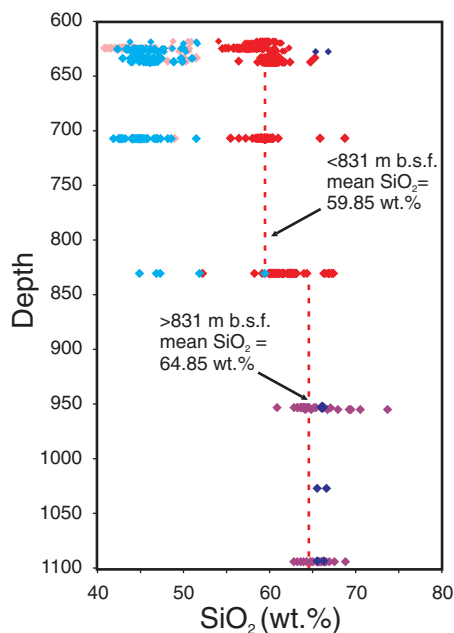


Figure 8. SiO_2 versus sample depth diagram, indicating a general correlation between depth and the SiO_2 content of glasses: altered rhyolitic-trachytic compositions occur prevalently above 709.19 m below seafloor (mbsf), whereas sample at 831.68 mbsf marks the passage toward rhyolitic glass compositions occurring between 953.28 mbsf and base of core. Symbols as in Figure 6.

in a range of environments (submarine and/or subglacial to subaerial) and fed by basaltic and trachytic-rhyolitic magmas.

Paleoenvironment Implications

Volcaniclastic deposits are an important component of sedimentary successions and are valuable paleoenvironmental indicators. In marine and glaciomarine environments, pyroclastic fall deposits may result from subaerial volcanic activity and particle settling through a water column or by direct transformation of gas-supported pyroclastic flow into a water-saturated gravity flow (Schneider et al., 2001). Primary volcaniclastic deposits can also originate from submarine volcanic activity ranging in styles from explosive to effusive (White, 2000). Resedimented volcaniclastic deposits may result from reworking and resedimentation of pyroclasts previously erupted on land (including supraglacial, englacial, and subglacial debris) or on sea ice.

Volcanic detritus is persistent and abundant throughout the AND-2A core, representing the dominant clast type in 9 of the 14 lithostrati-

graphic units (Panter et al., 2008). Apart from LSU 1 (Del Carlo et al., 2009), volcanic material within the uppermost half of the core (to 608.35 mbsf) consists mostly of lava, scoria, and pumice clasts dispersed in coarse-grained deposits (e.g., conglomerate, diamictite) and reworked glass in sandstone, siltstone, and mudstone. The absence of pyroclastic fall deposits and resedimented volcaniclastic deposits in the upper part of the core may be explained by a combination of (1) source, type, and intensity of volcanic activity, (2) ice extent and environmental conditions within the McMurdo Sound at the time of deposition, or (3) erosional processes.

During the period between ca. 17.1 and 11.5 Ma, when sediments were being deposited in the upper 600 m of the core (Di Vincenzo et al., 2010), volcanic activity in southern Victoria Land may have been less energetic (limited areal dispersion of ejecta), thus resulting in the lack of any discrete tephra beds at the coring site. Eruptions may have been prevalently submarine or subglacial and characterized by a limited dispersal of pyroclasts, as is typical for these types of eruptions. However, this hypothesis seems to be in contrast with the findings of Martin et al. (2010) that showed the presence of an intense and predominantly subaerial volcanic activity producing lava flows and pyroclastic deposits at Gandalf Ridge (18.7 ± 0.3 and 15.5 ± 0.5 Ma), Pinnacle Valley (15.4 ± 0.1 and 13.0 ± 0.3 Ma), and Mason Spur (12.9 ± 0.1 and 11.4 ± 0.2 Ma) that are located ~ 80 km from the coring site. In addition, this seems to be in conflict with findings of Marchant et al. (1996) and Lewis et al. (2007), who documented mafic to felsic ash layers in the Dry Valleys that are dated between 11 and 15 Ma. An alternative explanation is that the presence of thick ice sheets in the Ross Sea embayment, with grounding lines located north of the present-day positions, could have hampered the direct delivery of wind-driven volcanic materials to the coring site (glacial paleoenvironmental conditions). Sedimentological and isotopic studies of sedimentary records demonstrate that changes in environmental conditions occurred between ca. 17.1 and 11.5 Ma (Zachos et al., 2008; Passchier et al., 2011), and these were accompanied by strong ice sheet fluctuations with multiple cycles of advance and retreat that could possibly have allowed the deposition of pyroclastic fall deposits. Pyroclastic fall deposits and resedimented volcaniclastic deposits may have been eroded during the deposition of massive, coarse-grained deposits (diamictite and conglomerates) in subglacial to proglacial environments.

Volcanic material within the bottom half of the core, >600 mbsf, consists of dispersed lava clasts, scoria fragments, pumice, one pyroclas-

tic fall deposit, and at least 10 resedimented volcaniclastic deposits. Components forming the 6-cm-thick lapilli tuff at 640 mbsf, which is dated as 17.4 Ma (Di Vincenzo et al., 2010), were most likely transported in an eruptive ash cloud and deposited directly through the water column. This would only be possible if open marine or partly open marine conditions prevailed at the time (Fig. 9). Rounding and abrasion of dispersed pumice and scoria indicate that they spent some time as floating rafts prior to sinking, or transported on the seafloor prior to deposition, or underwent weathering and resedimentation prior to their final deposition (Fig. 9). Limited mixing with fragments from nonvolcanic material and imbrication of clasts parallel to sand laminae or oriented along the lee side of ripple cross-laminations suggest deposition by low-energy volcaniclastic bottom or turbidity currents. Resedimented pumice- and scoria-rich sandstone to lapillistone can be considered indicators of open-water conditions with limited sea ice, similar to the pyroclastic fall deposit at ~ 640 mbsf. Resedimented, strongly laminated, ash-rich mudstone to sandstone found at ~ 636 and ~ 1027 mbsf are comparable with deposits generated by suspension settling from ice-proximal, turbid, meltwater plumes (Ó Cofaigh and Dowdeswell, 2001, and references therein) observed in fjord environments, and more rarely, in high-latitude open marine settings. The absence of grain rounding, the preservation of fragile structures, and the low degree of post-eruptive sediment mixing with nonvolcanic detritus all indicate that no significant reworking has occurred. We suggest that these pyroclasts were transported in eruptive columns, dispersed by wind onto the ice (glaciers), and finally released to the water column during repeated melting events. We therefore conclude that deposition of resedimented, strongly laminated, ash-rich mudstone to sandstone occurred in a proglacial setting with generally open marine conditions. Similar depositional and dispersal processes have long been suggested for modern volcanogenic sediments in McMurdo Sound (Bentley, 1979; Barrett et al., 1983; Macpherson, 1987; Atkins and Dunbar, 2009).

CONCLUSIONS

The sedimentological, morphoscopic, petrological, and geochemical study of pyroclasts recovered in AND-2A core has provided information about their volcanic sources and eruptions styles and new insights into their environment of deposition. One pyroclastic fall deposit and several resedimented volcaniclastic deposits recovered in AND-2A core record an intense and recurrent history of volcanic

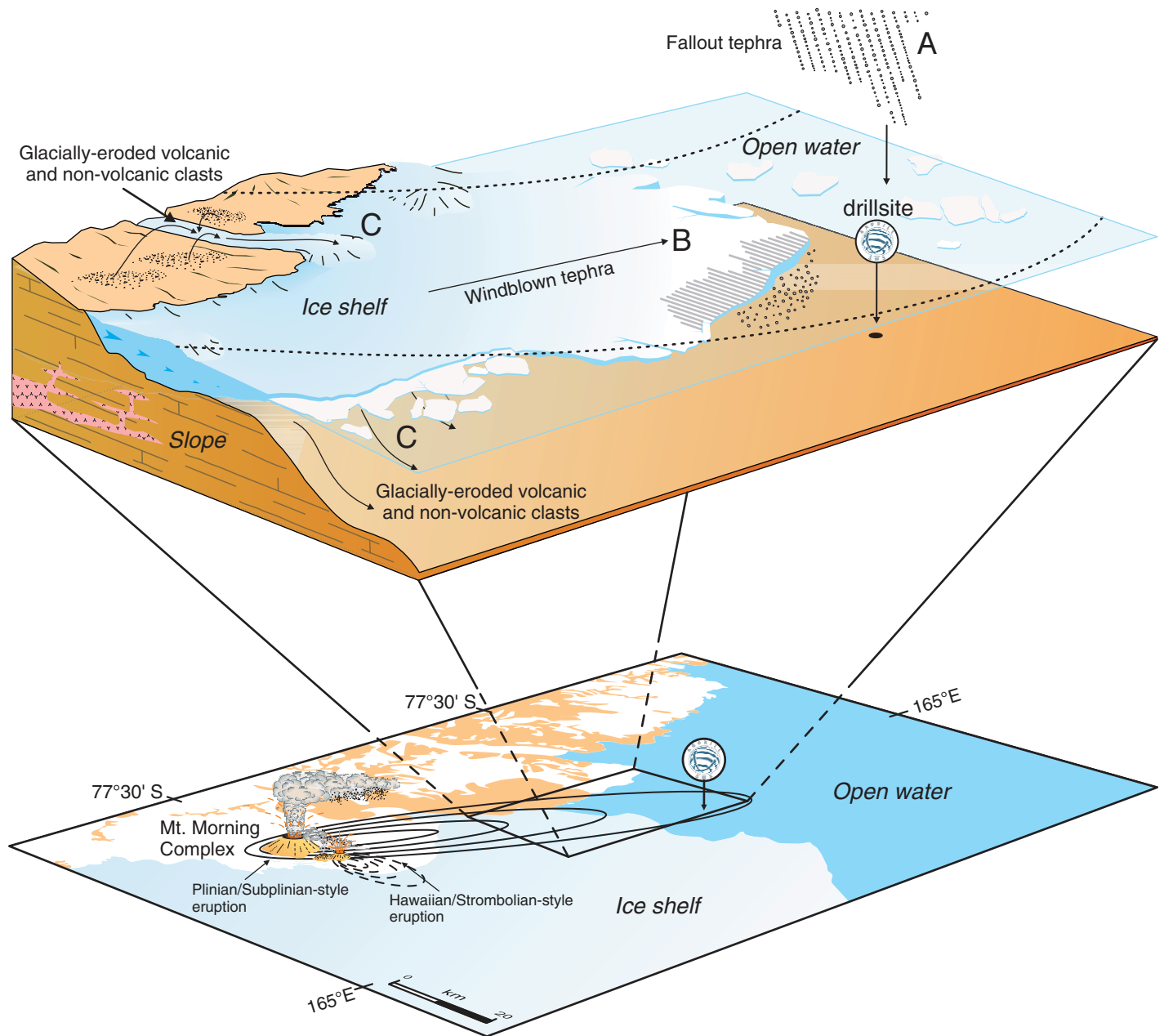


Figure 9. Schematic model illustrating possible eruptive, transport, and depositional processes of pyroclastic fall deposit, resedimented volcanoclastic deposits, and the volcanogenic sedimentary deposits. (A) Pyroclasts transported by a high eruptive column and finally deposited as pyroclastic fall deposit directly through the water column in open-water conditions. (B) Pumice and scoria clasts windblown over the ice and resedimented by suspension settling from ice-proximal turbid meltwater plumes or by low-energy volcanoclastic bottom and/or turbidity currents (resedimented volcanoclastic deposits). (C) Volcanic detritus deposited by glacialmarine processes (volcanogenic sedimentary deposits).

activity in the southern Victoria Land region during the Early Miocene. Two main explosive eruptive styles and magma compositions were recognized. Subplinian and Plinian eruptions involved trachytic to rhyolitic magmas, while Strombolian to Hawaiian eruptions were fed by basaltic to mugearitic magmas. In both cases the

occurrence of vesicle-free, blocky fragments indicates that hydromagmatic fragmentation processes were caused by the interaction of magmas with seawater and/or glacial meltwater within a glacialmarine environment. On the basis of the available geochemical and chronological data and using volcanological constraints, we

infer that the proto-Mount Morning and Mount Morning volcanoes located south of the drill site are the most likely volcanic sources. The sedimentological features of the volcanic units are interpreted to indicate that they were deposited in a proglacial setting with overall open-water marine conditions.

ACKNOWLEDGMENTS

The ANDRILL (Antarctic Geological Drilling) Program is a multinational collaboration between the Antarctic Programs of Germany, Italy, New Zealand, and the United States. Antarctica New Zealand is the project operator, and has developed the drilling system in collaboration with Alex Pyne at Victoria University of Wellington and Webster Drilling and Enterprises Ltd. Scientific studies are jointly supported by the U.S. National Science Foundation, New Zealand Foundation for Research Science and Technology, the Royal Society of New Zealand Marsden Fund, the Italian Antarctic Research Program, the German Research Foundation (Deutsche Forschungsgemeinschaft, DFG), and the Alfred Wegener Institute for Polar and Marine Research (Helmholtz Association of German Research Centers). Antarctica New Zealand supported the drilling team at Scott Base; Raytheon Polar Services supported the science team at McMurdo Station and the Cray Science and Engineering Laboratory. The ANDRILL Science Management Office at the University of Nebraska–Lincoln provided science planning and operational support. Di Roberto benefited from a postdoctoral grant from Programma Nazionale Ricerche in Antartide (PNRA). We are grateful to cochief F. Florindo and D. Harwood and the Science Team (<http://www.andrill.org>) of the Southern McMurdo Sound ANDRILL project. We thank A. Cavallo for the assistance during microprobe analyses, S. Petruschak for collecting samples of AND-2A core at Antarctic Marine Research Facility at Florida State University, and A.P. Martin and anonymous reviewers for their accurate and critical revisions of the manuscript.

REFERENCES CITED

- Acton, G., 25 others, and the ANDRILL-SMS Science Team, 2008, Preliminary integrated chronostratigraphy of the AND-2A core, ANDRILL Southern McMurdo Sound Project, in Harwood, D.M., et al., eds., Studies from the ANDRILL, Southern McMurdo Sound Project, Antarctica: Terra Antarctica, v. 15, p. 211–220.
- Armiienti, P., and Baroni, C., 1999, Cenozoic climatic change in Antarctica recorded by volcanic activity and landscape evolution: *Geology*, v. 27, p. 617–620, doi:10.1130/0091-7613(1999)027<0617:CCCIAR>2.3.CO;2.
- Armiienti, P., Civetta, I., Innocenti, F., Manetti, P., Tripodo, A., Villari, L., and Vita, G., 1991, New petrographical and geochemical data on Mt. Melbourne volcanic field, Northern Victoria Land, Antarctica: *Memorie della Società Geologica Italiana*, v. 46, p. 397–424.
- Armiienti, P., Messiga, B., and Vannucci, R., 1998, Sand provenance from major and trace element analyses of bulk rock and sand grains: *Terra Antarctica*, v. 5, p. 589–599.
- Armiienti, P., Tamponi, M., and Pompilio, M., 2001, Petrology and provenance of volcanic clasts, sand grains and tephra: *Terra Antarctica*, v. 8, p. 2–23.
- Armstrong, R.L., 1978, K-Ar dating: Late Cenozoic McMurdo Volcanic Group and Dry Valley glacial history, Victoria Land, Antarctica: *New Zealand Journal of Geology and Geophysics*, v. 21, p. 685–698, doi:10.1080/00288306.1978.10425199.
- Atkins, C.B., and Dunbar, G.B., 2009, Aeolian sediment flux from sea ice into Southern McMurdo Sound (SMS), Antarctica: *Global and Planetary Change*, v. 69, p. 133–141, doi:10.1016/j.gloplacha.2009.04.006.
- Barrett, P.J., 1987, Oligocene sequence cored at CIROS-1, western McMurdo Sound: *New Zealand: Antarctic Record*, v. 7, p. 1–17.
- Barrett, P.J., Pyne, A.R., and Macpherson, A.J., 1983, Observations of the sea floor of McMurdo Sound and Granite Harbour: *New Zealand: Antarctic Record*, v. 5, p. 16–22.
- Barrett, P.J., Fielding, C.R., and Sherwood, W., eds., 1998, Initial report on CRP-1, Cape Roberts Project, Antarctica: *Terra Antarctica*, v. 5, 187 p., hdl:10013/epic.28286.d001.
- Barrett, P.J., Sarti, M., and Sherwood, W., 2000, Studies from the Cape Roberts Project, Ross Sea, Antarctica. Initial reports on CRP-3: *Terra Antarctica*, v. 7, 209 p.
- Bentley, P.N., 1979, Characteristics and distribution of wind-blown sediment, Western McMurdo Sound, Antarctica [B.S. thesis]: Wellington, New Zealand, Victoria University of Wellington, 46 p.
- Carey, S., and Bursik, M., 2000, Volcanic plumes, in Sigurdsson, H., et al., eds., *Encyclopedia of volcanoes*: San Diego, California, Academic Press, p. 527–544.
- Cashman, K.V., Sturtevant, B., Papale, P., and Navon, O., 2000, Magmatic fragmentation, in Sigurdsson, H., et al., eds., *Encyclopedia of volcanoes*: San Diego, California, Academic Press, p. 421–430.
- Cooper, A.F., Adam, L.J., Coulter, R.F., Eby, G.N., and McIntosh, W.C., 2007, Geology, geochronology and geochemistry of a basanitic volcano, White Island, Ross Sea, Antarctica: *Journal of Volcanology and Geothermal Research*, v. 165, p. 189–216, doi:10.1016/j.jvolgeores.2007.06.003.
- Del Carlo, P., Panter, K.S., Bassett, K., Bracciali, L., Di Vincenzo, G., and Rocchi, S., 2009, The upper lithostratigraphic unit of ANDRILL AND-2A core (Southern McMurdo Sound, Antarctica): Local volcanic sources, paleoenvironmental implications and subsidence in the western Victoria Land Basin: *Global and Planetary Change*, v. 69, p. 142–161, doi:10.1016/j.gloplacha.2009.09.002.
- Di Roberto, A., Pompilio, M., and Wilch, T.I., 2010, Late Miocene submarine volcanism in ANDRILL AND-1B drill core, Ross Embayment, Antarctica: *Geosphere*, v. 6, p. 524–536, doi:10.1130/GES00537.1.
- Di Vincenzo, G., Bracciali, L., Del Carlo, P., Panter, K., and Rocchi, S., 2010, $^{40}\text{Ar}/^{39}\text{Ar}$ laser dating of volcanic products from the AND-2A core (ANDRILL Southern McMurdo Sound Project, Antarctica): *Bulletin of Volcanology*, v. 72, p. 487–505, doi:10.1007/s00445-009-0337-z.
- Esser, R.P., Kyle, P.R., and McIntosh, W.C., 2004, $^{40}\text{Ar}/^{39}\text{Ar}$ dating of the eruptive history of Mt. Erebus, Antarctica: Volcano evolution: *Bulletin of Volcanology*, v. 66, p. 671–686, doi:10.1007/s00445-004-0354-x.
- Fargo, A.J., McIntosh, W.C., Dunbar, N.W., and Wilch, T.I., 2008, $^{40}\text{Ar}/^{39}\text{Ar}$ geochronology of Minna Bluff, Antarctica: Timing of mid-Miocene glacial erosional events within the Ross Embayment: *Eos (Transactions, American Geophysical Union)*, v. 89, no. 53.
- Fielding, C.R., and Thomson, M.R.A., 1999, Studies from the Cape Roberts Project, Ross Sea Antarctica. Initial report on CRP-2/2A: *Terra Antarctica*, v. 6, 173 p.
- Fielding, C.R., Whittaker, J., Henrys, S.A., Wilson, T.J., and Naish, T.R., 2008, Seismic facies and stratigraphy of the Cenozoic succession in McMurdo Sound, Antarctica: Implications for tectonic, climatic and glacial history: *Palaeogeography, Palaeoclimatology, Palaeoecology*, v. 260, p. 8–29, doi:10.1016/j.palaeo.2007.08.016.
- Fielding, C.R., Browne, G.H., Field, B., Florindo, F., Harwood, D.M., Krissek, L.A., Levy, R.H., Panter, K.S., Passchier, S., and Pekar, S.F., 2011, Sequence stratigraphy of the ANDRILL AND-2A drillcore, Antarctica: A long-term, ice-proximal record of Early to Mid-Miocene climate, sea-level and glacial dynamism: *Palaeogeography, Palaeoclimatology, Palaeoecology*, v. 305, p. 337–351, doi:10.1016/j.palaeo.2011.03.026.
- Florindo, F., Harwood, D., and Levy, R., 2008, ANDRILL's success during the 4th International Polar Year: *Scientific Drilling*, v. 6, p. 29–31, doi:10.2204/iopd.sd.6.03.2008.
- Gamble, J.A., Barrett, P.J., and Adams, C.J., 1986, Basaltic clasts from Unit 8: *Bulletin of New Zealand*, v. 237, p. 145–152.
- Gifkins, C.C., Herrmann, W., and Large, R.R., 2005 eds., *Altered volcanic rocks: A guide to description*: University of Tasmania Centre for Ore Deposit Research, 275 p.
- Hambrey, M.J., and Barrett, P.J., 1993, Cenozoic sedimentary and climatic record, Ross Sea region, Antarctica, in Kennet, J.P., and Warnke, D.A., eds., *The Antarctic paleoenvironment: A perspective on global change: Part Two: American Geophysical Union Antarctic Research Series*, v. 60, p. 91–124, doi:10.1029/AR060p0091.
- Harwood, D.M., Florindo, F., Talarico, F., and Levy, R.H., eds., 2008, Studies from the ANDRILL, Southern McMurdo Sound Project, Antarctica: *Terra Antarctica*, v. 15, 253 p.
- Harwood, D.M., Florindo, F., Talarico, F., Levy, R.H., Kuhn, G., Naish, T., Niessen, F., Powell, R., Pyne, A., and Wilson, G., 2009, Antarctic drilling recovers stratigraphic records from the continental margin: *Eos (Transactions, American Geophysical Union)*, v. 90, p. 90–91, doi:10.1029/2009EO110002.
- Heiken, G.H., and Fisher, R.V., 2000, Water and magma can mix—A history of the concepts of hydrovolcanism (1819–1980), in Negendank, J.F.W., and Brüchmann, C., eds., *International Maar Conference: Germany: Terra Nostra*, v. 6, p. 165–189.
- Heiken, G.H., and Wohletz, K.H., 1985, *Volcanic ash*: Berkeley, University of California Press, 245 p.
- Heiken, G.H., and Wohletz, K., 1991, Fragmentation processes in explosive volcanic eruptions, in Fisher, R.V., and Smith, G., eds., *Sedimentation in volcanic settings: Society of Sedimentary Geology Special Publication* 45, p. 19–26.
- Houghton, B.F., and Wilson, C.J.N., 1989, A vesicularity index for pyroclastic deposits: *Bulletin of Volcanology*, v. 51, p. 451–462, doi:10.1007/BF01078811.
- Ishikawa, Y., Sawaguchi, T., Iwaya, S., and Horiuchi, M., 1976, Delineation of prospecting targets for Kuroko deposits based on modes of volcanism of underlying dacite and alteration haloes: *Mining Geology*, v. 26, p. 105–117.
- Klug, C., and Cashman, K.V., 1996, Permeability development in vesiculating magmas: Implications for fragmentation: *Bulletin of Volcanology*, v. 58, p. 87–100, doi:10.1007/s004450050128.
- Kyle, P.R., 1977, Mineralogy and glass chemistry of recent volcanic ejecta from Mt. Erebus, Ross Island, Antarctica: *New Zealand Journal of Geology and Geophysics*, v. 20, p. 1123–1146, doi:10.1080/00288306.1977.10420699.
- Kyle, P.R., 1981, Mineralogy and geochemistry of a basanite to phonolite sequence at Hut Point Peninsula, Antarctica, based on core from Dry Valley Drilling Project Drillholes 1, 2 and 3: *Journal of Petrology*, v. 22, p. 451–500, doi:10.1093/petrology/22.4.451.
- Kyle, P.R., 1982, Volcanic geology of the Pleiades, Northern Victoria Land, Antarctica, in Craddock, C., ed., *Antarctic geoscience*: Madison, University of Wisconsin Press, p. 747–754.
- Kyle, P.R., and Cole, J.W., 1974, Structural control of volcanism in the McMurdo Volcanic Group, Antarctica: *Bulletin of Volcanology*, v. 38, p. 16–25, doi:10.1007/BF02597798.
- Kyle, P.R., and Muncy, H.L., 1989, Geology and geochronology of McMurdo Volcanic Group rocks in the vicinity of Lake Morning, McMurdo Sound, Antarctica: *Antarctic Science*, v. 1, p. 345–350, doi:10.1017/S0954102089000520.
- Kyle, P.R., and 15 others, 1990, McMurdo Volcanic Group Western Ross embayment, in LeMasurier, W.E., and Thomson, J.W., eds., *Volcanoes of the Antarctic plate and southern oceans: American Geophysical Union Antarctic Research Series*, v. 48, p. 18–145, doi:10.1029/AR048p0018.
- Kyle, P.R., Moore, J.A., and Thirwall, M.F., 1992, Petrologic evolution of anorthoclase phonolite lavas at Mt. Erebus, Ross Island, Antarctica: *Journal of Petrology*, v. 33, p. 849–875, doi:10.1093/petrology/33.4.849.
- Large, R.R., Gemmill, J.B., Paulick, H., and Huston, D.L., 2001, The alteration box plot: A simple approach to understanding the relationship between alteration mineralogy and lithochemistry associated with volcanic-hosted massive sulfide deposits: *Economic Geology and the Bulletin of the Society of Economic Geologists*, v. 96, p. 957–971, doi:10.2113/96.5.957.
- LeMaitre, R.W., 1989, *A classification of igneous rocks and glossary of terms*: Oxford, Blackwell Science, 193 p.

Volcanic activity and paleoenvironment conditions in tephra layers of the AND-2A core

- Lewis, A.R., Marchant, D.R., Ashworth, A.C., Hemming, S.R. and Machlus, M.L., 2007, Major middle Miocene global climate change: Evidence from East Antarctica and the Transantarctic Mountains: *Geological Society of America Bulletin*, v. 119, p. 1449–1461, doi:10.1130B26134.1.
- Macpherson, A.J., 1987, The MacKay Glacier/Granite Harbour system (Ross Dependency, Antarctica). A study in nearshore glacial marine sedimentation [thesis]: Wellington, New Zealand, Victoria University of Wellington, 85 p.
- Mankinen, E.A., and Cox, A., 1988, Paleomagnetic investigation of some volcanic rocks from the McMurdo volcanic province, Antarctica: *Journal of Geophysical Research*, v. 93, p. 11,599–11,612, doi:10.1029/JB093iB10p11599.
- Marchant, D.R., Denton, G.H., Swisher, C.C., III, and Potter, N., Jr., 1996, Late Cenozoic Antarctic paleoclimate reconstructed from volcanic ashes in the Dry Valleys region of southern Victoria Land: *Geological Society of America Bulletin*, v. 108, p. 181–194, doi:10.1130/0016-7606(1996)108<0181:LCAPRF>2.3.CO;2.
- Maria, A., and Carey, S., 2002, Using fractal analysis to quantitatively characterize the shapes of volcanic particles: *Journal of Geophysical Research*, v. 107, p. 2283–2300, doi:10.1029/2001JB000822.
- Marsaglia, K.M., and Tazaki, K., 1992, Diagenetic trends in Leg 126 sandstones, *in* Tylor, B., et al., *Proceedings of the Ocean Drilling Program, Scientific results, Volume 126*: College Station, Texas, Ocean Drilling Program, p. 125–138.
- Martin, A.P., 2009, Mt. Morning, Antarctica: Geochemistry, geochronology, petrology, volcanology, and oxygen fugacity of the rifted Antarctic lithosphere [Ph.D. thesis]: Dunedin, New Zealand, University of Otago, 826 p.
- Martin, A., Cooper, A., and Dunlap, W., 2010, Geochronology of Mt. Morning, Antarctica: Two-phase evolution of a long-lived trachyte-basanite-phonolite eruptive center: *Bulletin of Volcanology*, v. 72, p. 357–371, doi:10.1007/s00445-009-0319-1.
- Mayewski, P.A., 1975, Glacial geology and late Cenozoic history of the Transantarctic Mountains, Antarctica: Columbus, Ohio State University, Institute of Polar Studies Report 56, 168 p.
- McIntosh, W.C., 1998, ⁴⁰Ar/³⁹Ar geochronology of volcanic clasts and pumice in CRP-1 core, Cape Roberts, Antarctica: *Terra Antarctica*, v. 5, p. 683–690.
- McIntosh, W.C., 2000, ⁴⁰Ar/³⁹Ar geochronology of tephra and volcanic clasts in CRP-2A, Victoria Land Basin, Antarctica: *Terra Antarctica*, v. 7, p. 621–630.
- McPhie, J., Doyle, M., and Allen, R.L., eds., 1993, *Volcanic textures: A guide to the interpretation of textures in volcanic rocks*: University of Tasmania, Centre for Ore Deposit and Exploration Studies, 198 p.
- Mercer, J.H., 1968, Glacial geology of the Reedy glacier area, Antarctica: *Geological Society of America Bulletin*, v. 79, p. 471–486, doi:10.1130/0016-7606(1968)79[471:GGOTRG]2.0.CO;2.
- Morrissey, M., Zimanowski, B., Wohletz, K., and Buettner, R., 2000, Phreatomagmatic fragmentation, *in* Sigurdsson, H., et al., eds., *Encyclopedia of volcanoes*: San Diego, California, Academic Press, p. 231–245.
- Müller, P., Schmidt-Thomé, M., Kreuzer, H., Tessensohn, F., and Vetter, U., 1991, Cenozoic peralkaline magmatism at the western margin of the Ross Sea, Antarctica: *Memorie della Societa Geologica Italiana*, v. 46, p. 315–336.
- Naish, T., Powell, R., and Levy, R.H., eds., 2007, *Studies from the ANDRILL, McMurdo Ice Shelf Project, Antarctica—Initial science report on AND-1B*: Terra Antarctica, v. 14, 328 p.
- Nardini, I., Armienti, P., Rocchi, S., Dallai, L., and Harrison, D., 2009, Sr-Nd-Pb-He-O isotope and geochemical constraints on the genesis of Cenozoic magmas from the West Antarctic Rift: *Journal of Petrology*, v. 50, p. 1359–1375, doi:10.1093/ptrology/egn082.
- Nyland, R., 2011, Evidence for early-phase explosive basaltic volcanism at Mt. Morning from glass-rich sediments in the ANDRILL AND-2A core and possible response to glacial cyclicity [M.S. thesis]: Bowling Green, Ohio, Bowling Green State University, 158 p.
- Nyland, R., Panter, K., Del Carlo, P., Di Vincenzo, G., Rocchi, S., Tiepolo, M., and Field, B., 2011, Geochemistry of Miocene glass in sediments from the AND-2A Core, McMurdo Sound, Antarctica: Magma petrogenesis and response to glacial unloading: AGU Fall Meeting, San Francisco, California, 5–9 December, Abstract V31F-2592.
- Ó Cofaigh, C., and Dowdeswell, J.A., 2001, Laminated sediments in glacial marine environments: Diagnostic criteria for their interpretation: *Quaternary Science Reviews*, v. 20, p. 1411–1436, doi:10.1016/S0277-3791(00)00177-3.
- Panter, K.S., and Winter, B., 2008, Geology of the side crater of the Erebus volcano, Antarctica: *Journal of Volcanology and Geothermal Research*, v. 177, p. 578–588, doi:10.1016/j.jvolgeores.2008.04.019.
- Panter, K.S., and 14 others, 2008, Petrologic and geochemical composition of the AND-2A core, ANDRILL Southern McMurdo Sound Project, Antarctica, *in* Harwood, D.M., et al., eds., *Studies from the ANDRILL, Southern McMurdo Sound Project, Antarctica: Terra Antarctica*, v. 15, p. 147–192.
- Parfitt, E.A., 2004, A discussion of the mechanisms of explosive basaltic eruptions: *Journal of Volcanology and Geothermal Research*, v. 134, p. 77–107, doi:10.1016/j.jvolgeores.2004.01.002.
- Passchier, S., Browne, G., Field, B., Fielding, C.R., Krissek, L.A., Panter, K., Pekar, S.F., and ANDRILL-SMS Science Team, 2011, Early and middle Miocene Antarctic glacial history from the sedimentary facies distribution in the AND-2A drill hole, Ross Sea, Antarctica: *Geological Society of America Bulletin*, v. 123, p. 2352–2365, doi:10.1130/B30334.1.
- Paulsen, T.S., and Wilson, T.J., 2009, Structure and age of volcanic fissures on Mount Morning: A new constraint on Neogene to contemporary stress in the West Antarctic Rift, southern Victoria Land, Antarctica: *Geological Society of America Bulletin*, v. 121, p. 1071–1088, doi:10.1130/B26333.1.
- Pompilio, M., Armienti, P., and Tamponi, M., 2001, Petrography, mineral composition and geochemistry of volcanic and subvolcanic rocks of CRP-3, Victoria Land Basin, Antarctica: *Terra Antarctica*, v. 8, p. 469–480.
- Rilling, S., Mukasa, S., Wilson, T., Lawver, L., and Hall, C., 2009, New determinations of ⁴⁰Ar/³⁹Ar isotopic ages and flow volumes for Cenozoic volcanism in the Terror Rift, Ross Sea, Antarctica: *Journal of Geophysical Research*, v. 114, B12207, doi:10.1029/2009JB006303.
- Rocchi, S., Armienti, P., D’Orazio, M., Tonarini, S., Wijbrans, J.R., and Di Vincenzo, G., 2002, Cenozoic magmatism in the western Ross Embayment: Role of mantle plume versus plate dynamics in the development of the West Antarctic Rift System: *Journal of Geophysical Research*, v. 107, 2195, doi:10.1029/2001JB000515.
- Sandroni, S., and Talarico, F.M., 2006, Analysis of clast lithologies from CIROS-2 core, New Harbour, Antarctica—Implications for ice flow directions during Pliocene-Pleistocene time: *Palaeogeography, Palaeoclimatology, Palaeoecology*, v. 231, p. 215–232, doi:10.1016/j.palaeo.2005.07.031.
- Schmidt-Thomé, M., Mueller, P., and Tessensohn, F., 1990, McMurdo Volcanic Group—western Ross Embayment: Malta Plateau: *Antarctic Research Series*, v. 48, p. 53–59.
- Schneider, J.L., Le Ruyet, A., Chanier, F., Buret, C., Ferriere, J., Proust, J.N., and Rosseel, J.B., 2001, Primary or secondary distal volcanoclastic turbidites: How to make the distinction? An example from the Miocene of New Zealand (Mahia Peninsula, North Island): *Sedimentary Geology*, v. 145, p. 1–22, doi:10.1016/S0037-0738(01)00108-7.
- Smellie, J.L., 1998, Sand grain detrital modes in CRP-1: Provenance variations and influence of Miocene eruptions on the marine record in the McMurdo Sound region: *Terra Antarctica*, v. 5, p. 579–587.
- Smellie, J.L., 2000, Subglacial eruptions, *in* Sigurdsson, H., et al., eds., *Encyclopedia of volcanoes*: San Diego, California, Academic Press, p. 403–418.
- Talarico, F., and Sandroni, S., 2011, Early Miocene basement clasts in ANDRILL AND-2A core and their implications for paleoenvironmental changes in the McMurdo Sound region (western Ross Sea, Antarctica): *Global and Planetary Change*, v. 78, p. 23–35, doi:10.1016/j.gloplacha.2011.05.002.
- Talarico, F., Pace, D., and Sandroni, S., 2011, Amphibole-bearing metamorphic clasts in ANDRILL AND-2A core: A provenance tool to unravel the Miocene glacial history in the Ross Embayment (western Ross Sea, Antarctica): *Geosphere*, v. 7, p. 922–937, doi:10.1130/GES00653.1.
- Tauxe, L., Gans, P., and Mankinen, E.A., 2004, Paleomagnetism and ⁴⁰Ar/³⁹Ar ages from volcanics extruded during the Matuyama and Brunhes Chrons near McMurdo Sound, Antarctica: *Geochemistry Geophysics Geosystems*, v. 5, Q06H12, doi:10.1029/2003GC000656.
- Timms, C., 2006, Reconstruction of a grounded ice sheet in McMurdo Sound—Evidence from southern Black Island, Antarctica [M.S. thesis]: Dunedin, New Zealand, University of Otago, 146 p.
- Tonarini, S., Rocchi, S., Armienti, P., and Innocenti, F., 1997, Constraints on timing of Ross Sea rifting inferred from Cenozoic intrusions from northern Victoria Land, Antarctica, *in* Ricci, C.A., ed., *The Antarctic region: Geological evolution and processes*: Siena, Italy, Terra Antarctica, p. 511–521.
- White, J.D.L., 2000, Subaqueous eruption-fed density currents and their deposits: *Precambrian Research*, v. 101, p. 87–109, doi:10.1016/S0301-9268(99)00096-0.
- Wilch, T.I., Lux, D.R., Denton, G.H., and McIntosh, W.C., 1993, Minimal Pliocene–Pleistocene uplift of the dry valleys sector of the Transantarctic Mountains: A key parameter in ice-sheet reconstructions: *Geology*, v. 21, p. 841–844, doi:10.1130/0091-7613(1993)021<0841:MPPUOT>2.3.CO;2.
- Wilch, T.I., McIntosh, W.C., Panter, K.S., Dunbar, N.W., Smellie, J.L., Fargo, A., Scanlan, M., Zimmerer, M.J., Ross, J., and Bosket, M.E., 2008, Volcanic and glacial geology of the Miocene Minna Bluff Volcanic Complex, Antarctica: *Eos (Transactions, American Geophysical Union)*, v. 89, fall meeting supplement, abs. V11F-06.
- Wilch, T.I., Panter, K.S., McIntosh, W.C., Dunbar, N.W., Smellie, J.L., Fargo, A., Scanlan, M., Zimmerer, M.J., Ross, J., and Bosket, M.E., 2008, Volcanic and glacial geology of the Miocene Minna Bluff Volcanic Complex, Antarctica: *Eos (Transactions, American Geophysical Union)*, v. 89, fall meeting supplement, abs. V11F-06.
- Wright-Grassham, A.C., 1987, Volcanic geology, mineralogy and petrogenesis of the Discovery volcanic sub-province, southern Victoria Land, Antarctica [Ph.D. thesis]: Socorro, New Mexico Institute of Mining and Technology, 460 p.
- Zachos, J.C., Dickens, G.R., and Zeebe, R.E., 2008, An early Cenozoic perspective on greenhouse warming and carbon-cycle dynamics: *Nature*, v. 451, p. 279–283, doi:10.1038/nature06588.

Geosphere

Early Miocene volcanic activity and paleoenvironment conditions recorded in tephra layers of the AND-2A core (southern McMurdo Sound, Antarctica)

A. Di Roberto, P. Del Carlo, S. Rocchi and K.S. Panter

Geosphere 2012;8;1342-1355

doi: 10.1130/GES00754.1

Email alerting services

click www.gsapubs.org/cgi/alerts to receive free e-mail alerts when new articles cite this article

Subscribe

click www.gsapubs.org/subscriptions/ to subscribe to Geosphere

Permission request

click <http://www.geosociety.org/pubs/copyrt.htm#gsa> to contact GSA

Copyright not claimed on content prepared wholly by U.S. government employees within scope of their employment. Individual scientists are hereby granted permission, without fees or further requests to GSA, to use a single figure, a single table, and/or a brief paragraph of text in subsequent works and to make unlimited copies of items in GSA's journals for noncommercial use in classrooms to further education and science. This file may not be posted to any Web site, but authors may post the abstracts only of their articles on their own or their organization's Web site providing the posting includes a reference to the article's full citation. GSA provides this and other forums for the presentation of diverse opinions and positions by scientists worldwide, regardless of their race, citizenship, gender, religion, or political viewpoint. Opinions presented in this publication do not reflect official positions of the Society.

Notes

